The Final Measurement of ϵ'/ϵ from KTeV

E. Worcester
University of Chicago, Chicago, Illinois

We present precision measurements of the direct CP violation parameter, $Re(\epsilon'/\epsilon)$, the K_L-K_S mass difference, Δm, the K_S lifetime, τ_S, and the CPT tests, ϕ_{+-} and $\Delta\phi$, in neutral kaon decays. These results are based on the full dataset collected by the KTeV experiment at Fermi National Accelerator Laboratory during 1996, 1997, and 1999. This dataset contains ~15 million $K \to \pi^0\pi^0$ decays and ~69 million $K \to \pi^+\pi^-$ decays. We describe significant improvements to the precision of these measurements relative to previous KTeV analyses. We find $Re(\epsilon'/\epsilon) = [19.2 \pm 1.1(stat) \pm 1.8(syst)] \times 10^{-4}$, $\Delta m = (5269.9 \pm 12.3) \times 10^6\ \hbar s^{-1}$, and $\tau_S = (89.623 \pm 0.047) \times 10^{-12}$ s. We measure the phase $\phi_{+-} = (43.76 \pm 0.64)^\circ$ and the difference between the relative phases $\Delta\phi = (0.30 \pm 0.35)^\circ$; these results are consistent with CPT symmetry.

I. INTRODUCTION

Violation of CP symmetry occurs in the neutral kaon system in two different ways. The dominant effect is the result of an asymmetry in the mixing of K^0 and $\overline{K^0}$ such that K_L and K_S are not CP eigenstates. This effect is parameterized by ϵ and is called indirect CP violation. The other effect, called direct CP violation, occurs in the $K \to \pi\pi$ decay process and is parameterized by ϵ'. Direct CP violation affects the decay rates of $K \to \pi^+\pi^-$ and $K \to \pi^0\pi^0$ differently, so it is possible to measure the level of direct CP violation by comparing η_{+-} and η_{00}:

$$\begin{aligned}
\eta_{+-} &= \frac{A(K_L \to \pi^+\pi^-)}{A(K_S \to \pi^+\pi^-)} = \epsilon + \epsilon' \\
\eta_{00} &= \frac{A(K_L \to \pi^0\pi^0)}{A(K_S \to \pi^0\pi^0)} = \epsilon - 2\epsilon' \qquad (1) \\
Re(\epsilon'/\epsilon) &\approx \frac{1}{6}\left(\left|\frac{\eta_{+-}}{\eta_{00}}\right|^2 - 1\right).
\end{aligned}$$

Measurements of $\pi\pi$ phase shifts [1] show that, in the absence of CPT violation, the phase of ϵ' is approximately equal to that of ϵ. Therefore, $Re(\epsilon'/\epsilon)$ is a measure of direct CP violation and $Im(\epsilon'/\epsilon)$ is a measure of CPT violation.

For small $|\epsilon'/\epsilon|$, $Im(\epsilon'/\epsilon)$ is related to the phases of η_{+-} and η_{00} by

$$\begin{aligned}
\phi_{+-} &\approx \phi_\epsilon + Im(\epsilon'/\epsilon) \\
\phi_{00} &\approx \phi_\epsilon - 2Im(\epsilon'/\epsilon) \qquad (2) \\
\Delta\phi &\equiv \phi_{00} - \phi_{+-} \approx -3Im(\epsilon'/\epsilon)\ .
\end{aligned}$$

Experimental results have established that $Re(\epsilon'/\epsilon)$ is non-zero [2–5]. In 2003, KTeV reported $Re(\epsilon'/\epsilon) = (20.7 \pm 2.8) \times 10^{-4}$ based on data from 1996 and 1997[6]. We now report the final measurement of $Re(\epsilon'/\epsilon)$ from KTeV. The measurement is based on 85 million reconstructed $K \to \pi\pi$ decays collected in 1996 1997, and 1999. This full sample is two times larger than, and contains, the sample on which the previous results are based. We also present measurements of the kaon parameters Δm and τ_S, and tests of CPT symmetry based on measurements of $\Delta\phi$ and $\phi_{+-} - \phi_{SW}$.

For these results we have made significant improvements to the data analysis and the Monte Carlo simulation. The full dataset, including those data used in the previous analysis, has been reanalyzed using the improved reconstruction and simulation. These results supersede the previously published results from KTeV[6]. In this presentation, we will focus primarily on improvements to the neutral mode analysis which have reduced the systematic uncertainty in $Re(\epsilon'/\epsilon)$ relative to the previous KTeV result.

II. THE KTEV EXPERIMENT

The measurement of $Re(\epsilon'/\epsilon)$ requires a source of K_L and K_S decays, and a detector to reconstruct the charged ($\pi^+\pi^-$) and neutral ($\pi^0\pi^0$) final states. The strategy of the KTeV experiment is to produce two identical K_L beams, and then to pass one of the beams through a "regenerator." The beam that passes through the regenerator is called the regenerator beam, and the other beam is called the vacuum beam. The regenerator creates a coherent $|K_L\rangle + \rho\,|K_S\rangle$ state, where ρ, the regeneration amplitude, is a physical property of the regenerator. The regenerator is designed such that most of the $K \to \pi\pi$ decays downstream of the regenerator are from the K_S component. The charged spectrometer is the primary detector for reconstructing $K \to \pi^+\pi^-$ decays and the pure Cesium Iodide (CsI) calorimeter is used to reconstruct the four photons from $K \to \pi^0\pi^0$ decays. A Monte Carlo simulation is used to correct for the acceptance difference between $K \to \pi\pi$ decays in the two beams, which results from the very different K_L and K_S lifetimes. The measured quantities are the vacuum-to-regenerator "single ratios" for $K \to \pi^+\pi^-$ and $K \to \pi^0\pi^0$ decay rates. These single ratios are proportional to $|\eta_{+-}/\rho|^2$ and $|\eta_{00}/\rho|^2$, and the ratio of these two quantities gives $Re(\epsilon'/\epsilon)$ via Eq. 1.

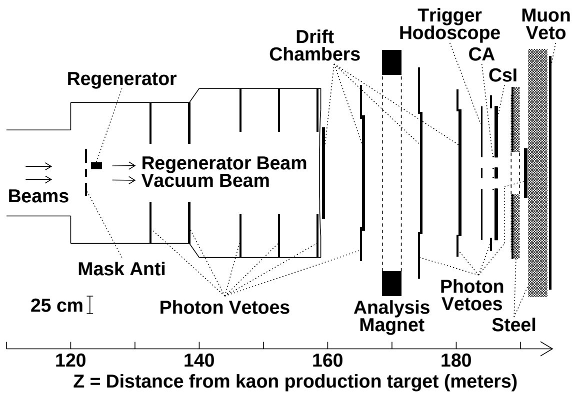

FIG. 1: The KTeV Detector

A. The KTeV Detector

The KTeV detector (Figure 1) consists of a charged spectrometer to reconstruct $K \to \pi^+\pi^-$ decays, a pure CsI electromagnetic calorimeter to reconstruct $K \to \pi^0\pi^0$ decays, a veto system to reduce backgrounds, and a three-level trigger to select events. Two virtually identical neutral kaon beams are incident on the detector; a movable active regenerator is placed in one of these beams to provide a coherent mixture of K_L and K_S. In this manner, we collect $K_L \to \pi\pi$ and $K_S \to \pi\pi$ decays simultaneously so that many systematic effects cancel in the ratios used to calculate $Re(\epsilon'/\epsilon)$.

The KTeV spectrometer consists of four drift chambers and a large dipole magnet. It measures the momenta of charged particles with an average resolution of 0.4%. The $K \to \pi^+\pi^-$ reconstruction achieves a z-vertex resolution of 5-30 cm and a mass resolution of 1.5 MeV/c^2. The CsI calorimeter measures the energies and positions of photons from the electromagnetic decay of the neutral pions in $K \to \pi^0\pi^0$ decays. It has an average energy resolution of 0.6%. The reconstructed decay vertex of the neutral pion is directly related to the energies of the photons:

$$Z_{\pi^0} = Z_{CsI} - \frac{r_{12}\sqrt{E_1 E_2}}{m_{\pi^0}}. \qquad (3)$$

The $K \to \pi^0\pi^0$ reconstruction achieves a z-vertex resolution of 20-30 cm and a mass resolution of 1.5 MeV/c^2.

B. Monte Carlo Simulation

KTeV uses a Monte Carlo (MC) simulation to calculate the detector acceptance and to model backgrounds to the signal modes. The very different K_L and K_S lifetimes lead to very different z-vertex distributions in the vacuum and regenerator beams. We determine the detector acceptance as a function of kaon decay vertex and energy including the effects of geometry, detector response, and resolutions. To help verify the accuracy of the MC simulation, we collect and study decay modes with approximately ten times higher statistics than the $K \to \pi\pi$ signal samples, such as $K_L \to \pi^\pm e^\mp \nu$ and $K_L \to \pi^0\pi^0\pi^0$.

Many improvements have been made to the MC simulation since the previous result was published in 2003[6]. We have improved the simulation of electromagnetic showers to include the effects of incident particle angles and to simulate the effects of wrapping and shims in the CsI calorimeter. We have improved the tracing of charged particles through the detector with more complete treatments of ionization energy loss, Bremsstrahlung, delta rays, and hadronic interactions in the drift chambers. We have also have updated a number of parameters that go into the kaon propogation and decay calculations.

The current Monte Carlo produces a significantly better simulation of electromagnetic showers in the CsI. Figure 2 shows the data-MC comparison of the fraction of energy in each of the 49 CsI crystals in a shower relative to the total reconstructed shower energy for electrons from $K_L \to \pi^\pm e^\mp \nu$ decays. The majority of the energy is deposited in the central crystal since the Moliere radius of CsI is 3.8 cm. These particular plots are made for 16-32 GeV electrons with incident angles of 20-30 mrad, but the quality of agreement is similar for other energies and angles. The data-MC disagreement improves from up to 15% for the 2003 MC to less than 5% for the current MC. This improvement in the modeling of electromagnetic shower shapes leads to important reductions in the systematic uncertainties associated with the reconstruction of photon showers from $K \to \pi^0\pi^0$ decays.

III. DATA ANALYSIS

The $K \to \pi^+\pi^-$ analysis consists primarily of the reconstruction of tracks in the spectrometer. The vertices and momenta of the tracks are used to calculate kinematic quantities describing the decay. The $K \to \pi^+\pi^-$ invariant mass distributions for each beam are shown in Figure 3.

To reconstruct $K \to \pi^0\pi^0$ decays, we measure the energies and positions of each cluster of energy in the CsI. A number of corrections are then made to the measured particle energies based on our knowledge of the CsI performance and the reconstruction algorithm. The precision of the CsI energy and position reconstruction is crucial to the $K \to \pi^0\pi^0$ analysis and has been improved significantly since the previous publication. We use the cluster positions and energies along with the known pion mass to determine which pair of photons is associated with which neutral pion from the kaon decay and calculate the decay

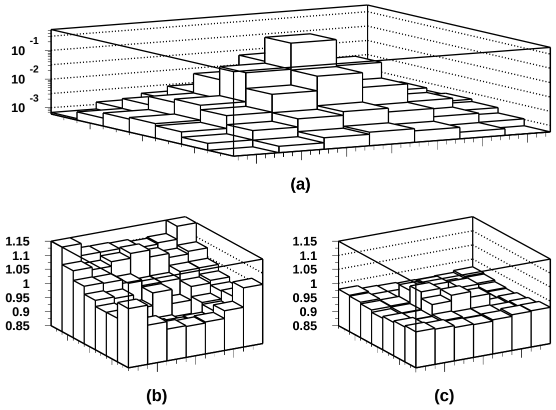

FIG. 2: Data-MC comparison of fraction of energy in each of the 49 CsI crystals in an electron shower. (a) The fraction of energy in each of the 49 CsI crystals in an electron shower for data. (b) 2003 data/MC ratio (c) current data/MC ratio

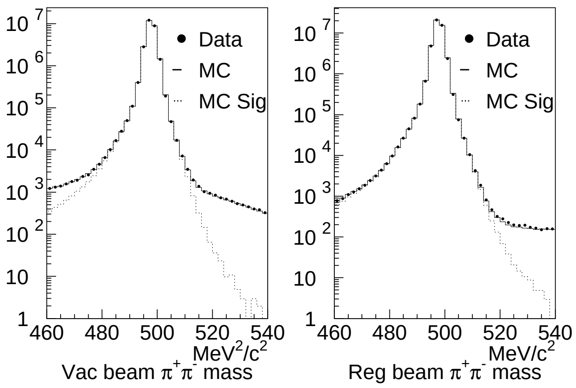

FIG. 3: $\pi^+\pi^-$ invariant mass distribution for $K \to \pi^+\pi^-$ candidate events. The data distribution is shown as dots, the $K \to \pi^+\pi^-(\gamma)$ signal MC (MC Sig) is shown as dotted histogram and the sum of signal and background MC is shown as a solid histogram.

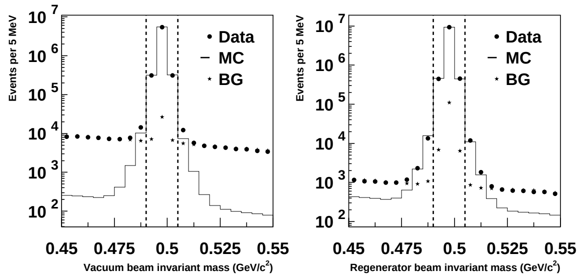

FIG. 4: $K \to \pi^0\pi^0$ $m_{\pi^0\pi^0}$ distributions for for data and MC in the vacuum (left) and regenerator (right) beams. The dashed lines indicate our cuts.

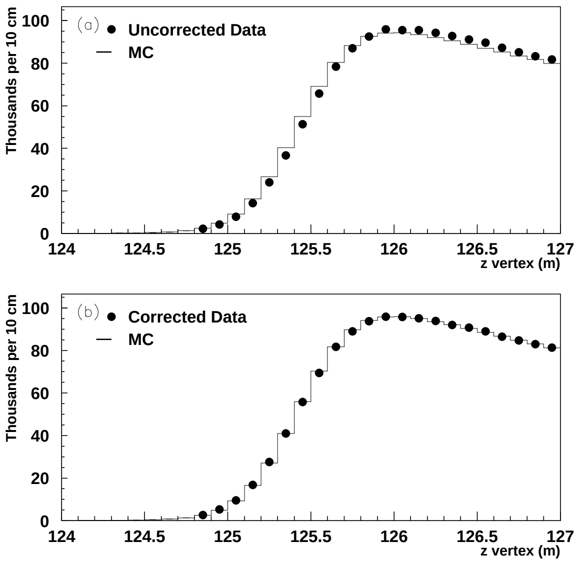

FIG. 5: Regenerator beam $K \to \pi^0\pi^0$ z-vertex distribution near the regenerator for 1999 data and Monte Carlo. (a) Uncorrected data. (b) Data with energy scale correction applied.

vertex, the center of energy, and the $\pi^0\pi^0$ invariant mass. The $K \to \pi^0\pi^0$ invariant mass distributions for each beam are shown in Figure 4.

For $K \to \pi^0\pi^0$ decays, the z vertex is determined using only the positions and energies of the four photons in the final state. Therefore, the measured z vertex is dependent upon the absolute energy scale of the CsI calorimeter. The energy scale is set using electrons from $K_L \to \pi^\pm e^\mp \nu$ decays. A small residual energy scale mismatch between data and Monte Carlo is removed by adjusting the energy scale in data such that the sharp edge in the z-vertex distribution at the regenerator matches between data and Monte Carlo as shown in Figure 5. The final energy scale adjustment for 1997 data is shown as a function of kaon energy in Figure 6; the average size of the correction is $\sim$0.04%. As a result of improvements to the simulation and reconstruction of clusters, the required energy scale adjustment is smaller and less dependent on kaon energy for low kaon energies than in the previous analysis.

Backgrounds to the $K \to \pi\pi$ signal modes are simulated using the Monte Carlo, normalized to the data, and subtracted. In this analysis, we use decays from coherently regenerated kaons only; diffractive and inelastic scattering in the regenerator is treated as background. Backgrounds contribute less than 0.1% of $K \to \pi^+\pi^-$ data and about 1% of $K \to \pi^0\pi^0$ data.

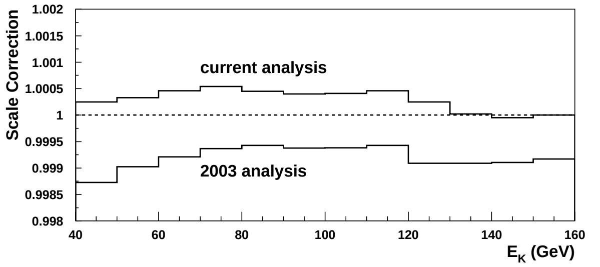

FIG. 6: Change in the final energy scale adjustment relative to the 2003 analysis. The dashed line represents no data-MC mismatch.

Table I summarizes the systematic uncertainties on $Re(\epsilon'/\epsilon)$. We describe the procedure for evaluating several important systematic uncertainties below.

Source	Error on $Re(\epsilon'/\epsilon)$ $(\times 10^{-4})$	
	$K \to \pi^+\pi^-$	$K \to \pi^0\pi^0$
Trigger	0.23	0.20
CsI cluster reconstruction	—	0.75
Track reconstruction	0.22	—
Selection efficiency	0.23	0.34
Apertures	0.30	0.48
Acceptance	0.57	0.48
Backgrounds	0.20	1.07
MC statistics	0.20	0.25
Total	0.81	1.55
Fitting	0.31	
Total	1.78	

TABLE I: Summary of systematic uncertainties in $Re(\epsilon'/\epsilon)$.

Acceptance: We use the Monte Carlo simulation to estimate the acceptance of the detector in momentum and z-vertex bins in each beam. We evaluate the quality of this simulation by comparing energy-reweighted z-vertex distributions in the vacuum beam between data and Monte Carlo. We fit a line to the data-MC ratio of the z-vertex distributions and call the slope of this line, s, the acceptance "z-slope." A z-slope affects the value of $Re(\epsilon'/\epsilon)$ by producing a bias between the regenerator and vacuum beams because of the very different z-vertex distributions in the two beams; we use the known difference of the mean z values for the vacuum and regenerator beams along with the measured z-slope to evaluate the systematic error on $Re(\epsilon'/\epsilon)$.

Figure 7 shows the measured z-slopes for the full $K_L \to \pi^+\pi^-$, $K_L \to \pi^\pm e^\mp \nu$, $K_L \to \pi^0\pi^0$, and $K_L \to \pi^0\pi^0\pi^0$ event samples. We use the $\pi^+\pi^-$ z-slope to set the systematic uncertainty and measure

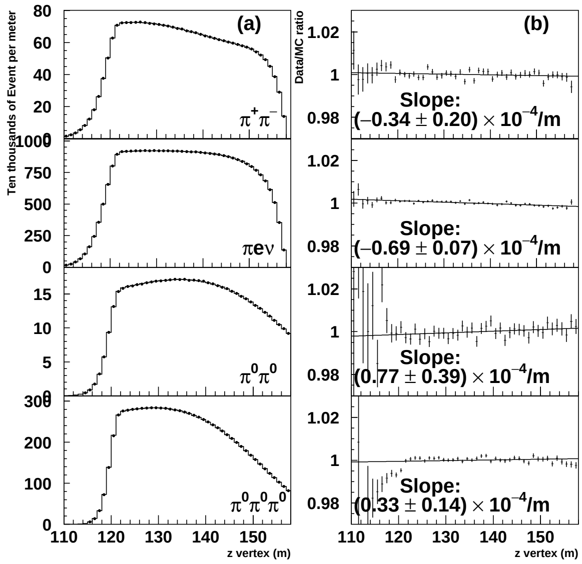

FIG. 7: Comparison of the vacuum beam z distributions for data (dots) and MC (histogram). The data-to-MC ratios on the right are fit to a line, and the z-slopes (see text) are shown. All distributions are for the full data sample used in this analysis.

the $\pi^\pm e^\mp \nu_e$ z-slope as a crosscheck. For neutral mode, we use the high statistics $\pi^0\pi^0\pi^0$ mode to set the systematic uncertainty because it has the same type of particles in the final state as $\pi^0\pi^0$ and is more sensitive than $\pi^0\pi^0$ to potential problems in the reconstruction due to close clusters, energy leakage at the CsI edges, and low photon energies.

Energy Scale: The final energy scale adjustment ensures that the energy scale matches between data and MC at the regenerator edge, but we must check whether the data and MC energy scales remain matched for the full length of the decay volume. We check the energy scale at the downstream end of the decay region by studying the z-vertex distribution of $\pi^0\pi^0$ pairs produced by hadronic interactions in the vacuum window in data and MC. To verify that this type of production has a comparable energy scale to $K \to \pi^0\pi^0$, we also study the z-vertex distribution of hadronic $\pi^0\pi^0$ pairs produced in the regenerator. The data-MC comparisons of reconstructed z vertex for these samples are shown in Figure 8.

To convert these shifts to an uncertainty in $Re(\epsilon'/\epsilon)$, we consider a linearly varying energy scale distortion such that no adjustment is made at the regenerator edge and the z shift at the vacuum window is that measured by the hadronic vacuum window sample. The average energy scale distortion we apply is shown by the hatched region in Figure 8. We rule out energy scale distortions that vary non-linearly as a function of z vertex as they introduce data-MC discrepancies in

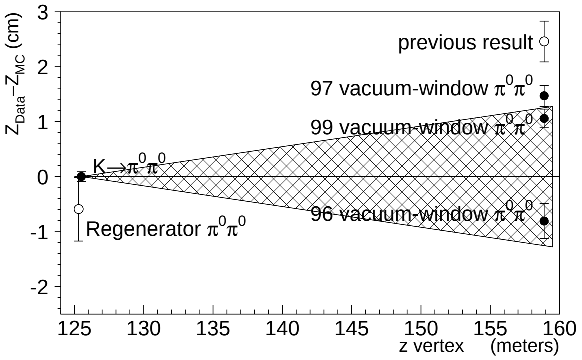

FIG. 8: Energy scale tests at the regenerator and vacuum window. The difference between the reconstructed z positions for data and MC is plotted for the $K \to \pi^0\pi^0$, regenerator $\pi^0\pi^0$, and vacuum window $\pi^0\pi^0$ samples. The solid point at the regenerator edge is the $K \to \pi^0\pi^0$ sample; there is no difference between data and MC by construction. The open point at the regenerator edge is the average shift of the regenerator $\pi^0\pi^0$ samples for all three years. The points at the vacuum window are the shifts for the vacuum window samples for each year separately. The hatched region shows the range of data-MC shifts covered by the total systematic uncertainty from the energy scale. For reference, the data-MC shift at the vacuum window from the 2003 analysis is also plotted.

other distributions. The systematic error on $Re(\epsilon'/\epsilon)$ due to uncertainties in the $K \to \pi^0\pi^0$ energy scale is $0.65{\times}10^{-4}$; this is a factor of two smaller than in the previous analysis.

Energy Non-linearity: Some reconstructed quantities in the analysis do not depend on the CsI energy scale, but are sensitive to energy non-linearities. To evaluate the effect of energy non-linearities on the reconstruction, we study the way the reconstructed kaon mass varies with reconstructed kaon energy, kaon z vertex, minimum cluster separation, and incident photon angle. Data-MC comparisons for these distributions for the 1999 data sample are shown in Figure 9. To measure any bias resulting from the nonlinearities that cause the small data-MC differences seen in these distributions, we investigate adjustments to the cluster energies that improve the agreement between data and MC in the plot of reconstructed kaon mass vs kaon energy. We find that a 0.1%/100 GeV distortion produces the best data-MC agreement for the 1997 and 1999 datasets. Figure 10 shows the improvement in data-MC agreement with this distortion applied to 1999 data. The data-MC agreement in the reconstructed kaon mass as a function of kaon energy has been significantly improved compared to the previous analysis in which a 0.7%/100 GeV distortion was required for 1997 data.

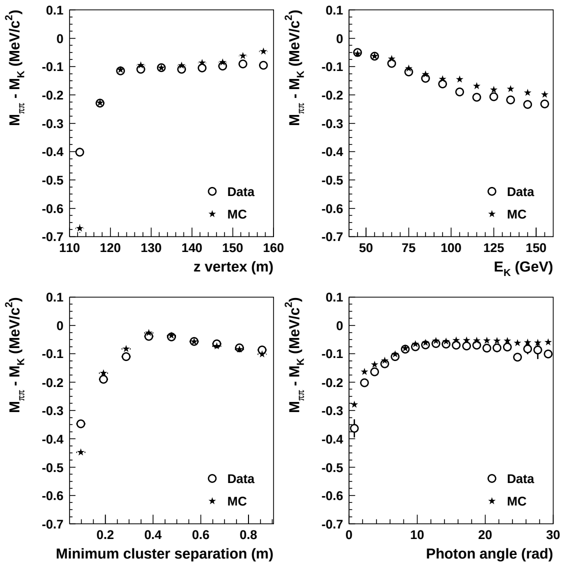

FIG. 9: Comparisons of the reconstructed kaon mass vs z-vertex (top left), kaon energy (top right), minimum cluster separation (bottom left), and photon angle (bottom right) for 1999 data and MC. The values plotted are the difference between the reconstructed kaon mass for each bin and the nominal PDG kaon mass.

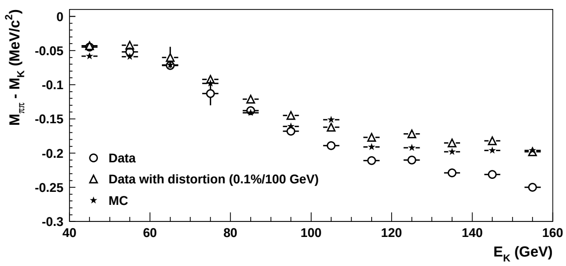

FIG. 10: Effect of 0.1%/100 GeV distortion on M_K vs E_K for 1999 data. The values plotted are the difference between the reconstructed kaon mass for each bin and the nominal PDG kaon mass.

IV. RESULTS

The final KTeV measurement of $Re(\epsilon'/\epsilon)$ for the full 1996, 1997, and 1999 combined dataset is:

$$Re(\epsilon'/\epsilon) = [19.2 \pm 1.1(stat) \pm 1.8(syst)] \times 10^{-4} \quad (4)$$

$$= [19.2 \pm 2.1] \times 10^{-4}. \quad (5)$$

We perform several checks of our result by breaking the data into subsets and checking the consistency of the $Re(\epsilon'/\epsilon)$ result. To check for any time dependence,

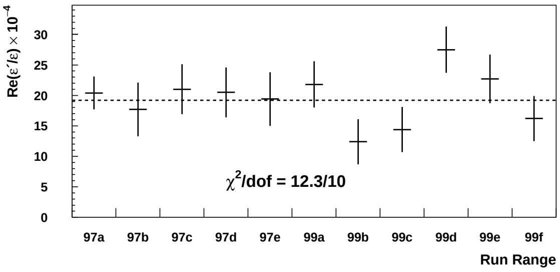

FIG. 11: $Re(\epsilon'/\epsilon)$ in subsets of the data sample. Each point is statistically independent. The dashed line indicates the value of $Re(\epsilon'/\epsilon)$ for the full data sample. The 97a run range includes the 1996 $K \to \pi^0\pi^0$ data.

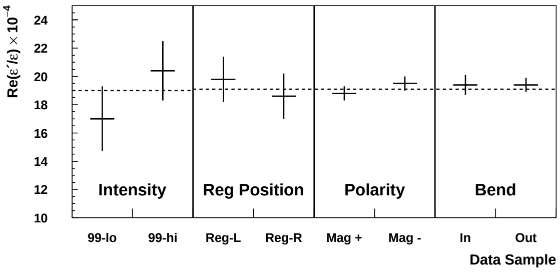

FIG. 12: $Re(\epsilon'/\epsilon)$ consistency with beam intensity, regenerator position, magnet polarity, and track bend. The low and high intensity samples are from 1999 only and have average rates of $\sim 1 \times 10^{11}$ protons/s and $\sim 1.6 \times 10^{11}$ protons/s, respectively. Reg-left and reg-right refer to the position of the regenerator beam in the detector. Mag+ and Mag- are the magnet polarity and in/out are the bend of the tracks in the magnet. In each of these subsets the $K \to \pi^0\pi^0$ sample is common to both fits; the errors are estimated by taking the quadrature difference with the error for the full dataset. The dashed lines indicate the value of $Re(\epsilon'/\epsilon)$ in the appropriate full data sample.

we break the data into 11 run ranges with roughly equal statistics. We divide the data in half based on beam intensity, regenerator position, magnet polarity, and direction in which the tracks bend in the magnet. We check for dependence of the result on kaon momentum by breaking the data into twelve 10 GeV/c momentum bins. The $Re(\epsilon'/\epsilon)$ results for these tests are shown in Figures 11, 12, and 13. We find consistent results in all of these subsamples.

We also measure the kaon parameters τ_S, Δm, ϕ_ϵ, $Re(\epsilon'/\epsilon)$, and $Im(\epsilon'/\epsilon)$ in a single, z-binned fit. The systematic uncertainties are evaluated using a procedure identical to that used for the $Re(\epsilon'/\epsilon)$ measurement. CPT invariance is imposed *a posteriori* including the total errors of the parameters with their correlations to obtain a precise measurement of Δm and τ_S. The results are:

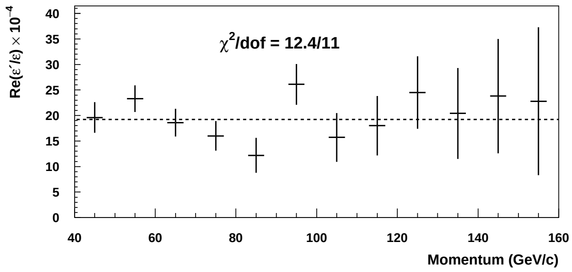

FIG. 13: $Re(\epsilon'/\epsilon)$ in 10 GeV/c momentum bins. The dashed line indicates the value for the full data sample.

$$\begin{aligned}
\Delta m\,|_{\rm cpt} &= [5269.9 \pm 12.3] \times 10^{-12}\ \text{s}, \\
\tau_S\,|_{\rm cpt} &= [89.623 \pm 0.047] \times 10^{6}\hbar/\text{s}, \\
\phi_{+-} &= [43.76 \pm 0.64]^\circ, \\
\phi_{00} &= [44.06 \pm 0.68]^\circ, \\
\delta\phi &= \phi_\epsilon - \phi_{SW} = [0.40 \pm 0.56]^\circ, \\
\Delta\phi &= -3Im(\epsilon'/\epsilon) = [0.30 \pm 0.35]^\circ.
\end{aligned} \tag{6}$$

Acknowledgments

We gratefully acknowledge the support and effort of the Fermilab staff and the technical staffs of the participating institutions. This work was supported in part by the U.S. Department of Energy, The National Science Foundation, and the Ministry of Education and Science in Japan.

[1] W. Ochs, πN Newsletter 3, 25 (1991).
[2] L.K. Gibbons et al. (E731), Phys. Rev. Lett. 70, 1203 (1993).
[3] G.D. Barr et al. (NA31), Phys. Lett. B317, 223 (1993).
[4] A. Alavi-Harati et al. (KTeV), Phys. Rev. Lett. 83, 22 (1999).
[5] A. Lai et al. (NA48), Eur Phys. J. C 22, 231 (2001).
[6] A. Alavi-Harati et al. (KTeV), Phys. Rev. D67, 012005 (2003).